Eur. Phys. J. Special Topics **166**, 151–154 (2009)

DOI: 10.1140/epjst/e2009-00897-7

THE EUROPEAN PHYSICAL JOURNAL
SPECIAL TOPICS

Regular Article

Switching wetting morphologies in triangular grooves

K. Khare[1,a], M. Brinkmann[1], B.M. Law[2], S. Herminghaus[1], and R. Seemann[1]

[1] Max-Planck-Institute for Dynamics and Self-Organization, 37073 Goettingen, Germany
[2] Physics Department, Kansas State University, Manhattan, KS 66506-2601, USA

Abstract. Static wetting morphologies in grooves with triangular cross section are studied here. Using the electrowetting effect, we can switch between different equilibrium morphologies and transport liquid along prefabricated grooves. The particular filling and drainage behavior in triangular grooves is discussed in terms of the groove geometry.

1 Introduction

Liquids generally prefer to wet wedges and grooves [1–3]. Only for large contact angle, the liquid will form drop-like structures almost irrespective of the underlying topography. Provided the contact angle θ of the liquid is sufficiently small, the liquid will follow the symmetry of the substrate. For very small contact angles even morphologies with negative Laplace pressure can be found [2–4]. This is in sharp contrast to planar (chemically structured) substrates where liquid exclusively forms wetting morphologies with positive Laplace pressure. When combined with a technique that allows us to vary the contact angle, we can switch between different equilibrium wetting morphologies and thus transport liquid along prefabricated grooves.

In this article we explore static polystyrene (PS) wetting morphologies in triangular grooves investigated by atomic force microscopy (AFM). Furthermore, the switching behavior of aqueous drops is studied by continuously varying the apparent contact angle using electrowetting on dielectric (EWOD) [5–8].

2 Experiments

Grooves with triangular cross section and width, w, ranging from $2\,\mu$m to $20\,\mu$m were fabricated in silicon (Si) using standard photolithography. The resulting opening angle is $\alpha = 70.6°$. For convenience, we will further refer to the wedge angle $\psi = 90° - \alpha/2$. For the electrowetting experiments, an oxide layer of thickness $d = (1.00 \pm 0.15)\,\mu$m was thermally grown into the grooved substrates.

Equilibrium wetting morphologies were formed exposing the grooved substrates to oversaturated vapor of short chain PS ($M_w = 1.89\,$kg/mol) for several hours. After cooling, the PS structures freeze and were imaged by AFM. The contact angle of the PS was modified by hydrophobizing the substrates with a self-assembled monolayer of semifluorinated trichlorosilane, $[F(C_2F)_8(CH_2)_2SiCl_3]$. To fine tune the wettability, a subsequent oxygen plasma treatment was performed [3].

[a] e-mail: krishnacharya@ds.mpg.de

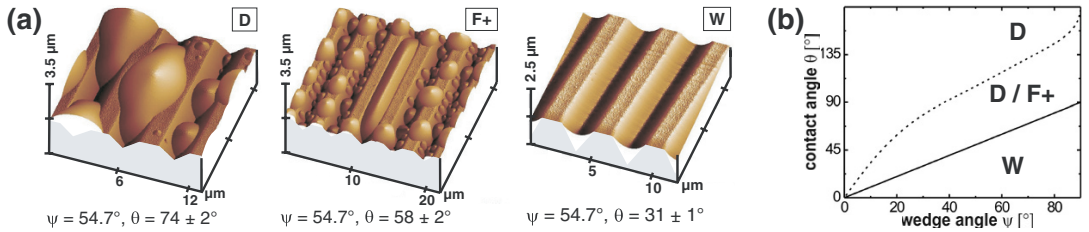

Fig. 1. Liquid morphologies in triangular grooves; (a) AFM images of PS morphologies condensed from the vapor phase. (b) Analytically calculated morphology diagram for triangular grooves.

For the EWOD experiments, the substrates were hydrophobized with a self-assembled monolayer of OTS (octadecyltrichlorosilane) molecules [9]. The conducting liquid used for all electrowetting experiments was a mixture of water, glycerol, and Sodium Chloride (salt) in the weight ratio of 17:80:3, which is hygroscopically stable against volume change in typical lab conditions [10]. Bulk conductivity of this solution is $\sigma_{\mathrm{bulk}} = (0.11 \pm 0.04)\,\mathrm{S/m}$ as measured by a "Ecoscan-Con5" conductometer. To exclude electrochemical effects, an AC voltage with frequencies ranging from $\omega = 1\,\mathrm{kHz}$ to $20\,\mathrm{kHz}$ were used. The apparent contact angle of the aqueous solution could be tuned from about 83° without any voltage applied, down to about 45° for an applied voltage of 100 V.

3 Results and discussions

In the limit of large liquid volumes three different wetting morphologies can be found in triangular grooves as shown in Fig. 1(a). It comprises localized drops (D), elongated filaments with positive Laplace pressure (F+) and liquid wedges with negative Laplace pressure (W). Figure 1(b) shows the morphology diagram for triangular grooves. Depending on wettability and geometry of the groove either localized drops (D) or liquid wedges (W) can be found as globally stable morphologies. The boundary line is given by $\theta = \psi$ [11,12]. For intermediate contact angle larger that ψ, elongated liquid filaments with positive mean curvature (F+) can be additionally found as locally stable structures.

Depositing the aqueous solution on the OTS coated, triangular grooved substrate, the liquid will form a drop-like morphology. As we decrease the contact angle of the liquid by applying a voltage between the drop and the silicon substrate, the apparent contact angle eventually crosses the boundary at $\theta = \psi$ and the liquid imbibes the grooves.

The series of optical micrographs displayed in Fig. 2(a) illustrates a typical groove filling experiment. The length of the filaments, l, clearly shows a threshold behavior as a function of applied voltage, U_0, cf. Fig. 2(b). This threshold voltage nicely agrees with the threshold contact angle as expected from the morphology diagram [4]. For further increasing U_0, the length of the filament further advances into the groove. The reason for the finite length of the filament is the ohmic resistance of the wetting liquid. This competes with the capacitive resistance of the insulating layer at the frequency of the applied AC voltage. Thus the voltage across the dielectric layer drops along the liquid filament, and the apparent ([13]) contact angle correspondingly increases along the filament. The voltage at the tip of the filament always equals the threshold voltage for groove filling [10].

The voltage drop along a liquid filament can be described by a transmission line model by considering the filament as a conducting material of constant cross section surrounded by an insulating layer [10]. Thus an analytical expression between the applied voltage at the drop, U_0, and the length of the liquid filament, l, can thus be derived:

$$U_0 = U_T \sqrt{\cosh^2(l/\lambda) - \sin^2(l/\lambda)}; \qquad \lambda = \sqrt{\frac{4\pi d\sigma}{\omega\varepsilon}\frac{w\sin\psi}{4}}. \tag{1}$$

Here, U_T is the threshold voltage for the groove filling, and ε is the permittivity of silicon dioxide. The natural length of the corresponding differential equation, λ, is composed of two

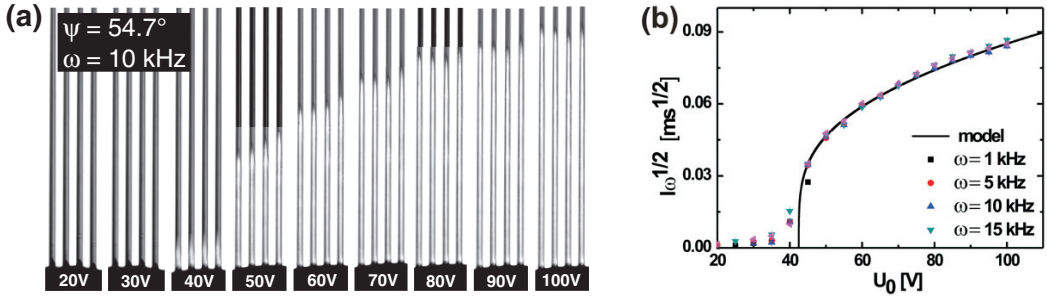

Fig. 2. (a) Top-view of a droplet of liquid (dark object at the bottm) imbibing grooves with triangular cross section for different voltages. (b) Master curve for the length of the liquid filament as function of the applied voltage for different frequencies. The solid line was obtained by numerically fitting Eq. (1) to the experimental data.

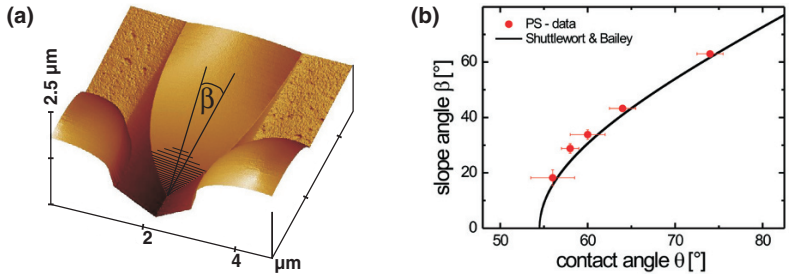

Fig. 3. (a) AFM micrograph showing the terminal part of the meniscus of a PS filament (F+) in a triangular groove. (b) Slope angle β as a function of the contact angle θ.

characteristic length scales of our system: $4\pi d\sigma/(\omega\varepsilon)$ representing the electrical properties of the material, and a geometrical length scale that is the ratio of the area of the cross section divided by the wetted surface area, $(w \sin\psi)/4$ [4,10].

If we re-scale the measured filament length according to the frequency dependence of $\lambda \propto \sqrt{1/\omega}$, all data collapse on a single master curve as shown in Fig. 2(b). Equation (1) is numerically fitted to the experimental data (solid line in Fig. 2(b) using the experimentally determined parameters as input parameters. The conductivity of the liquid is the only fitting parameter and was extracted to $\sigma_{\text{fit}} = 0.023 \pm 0.002\,\text{S/m}$ [4]. In contrast to rectangular grooves [10], we cannot reach a quantitative agreement between σ_{fit} and σ_{bulk}.

To explain this, we have to understand the filling behavior in more detail. For this reason we go back to the static wetting morphologies: It was first noted by Shuttleworth and Bailey [14] that the tip of a liquid filament in triangular grooves becomes more and more pointed as the contact angle θ reaches the wedge angle ψ. In their analysis, they assumed that the terminal part of the meniscus becomes asymptotically a plane approaching the tip and they used the slope angle of that plane, β, to characterize the tip shape, Fig. 3(a). By elementary geometry they derived a relation $\cos\beta \cos\psi = \cos\theta$ for the range $\theta > \psi$ shown as solid line in Fig. 3(b). The experimental data points, measured by AFM, for PS wetting morphologies agree well with the Shuttleworth prediction. This particular tip shape as function of the contact angle has some important repercussions on the filling and drainage behavior: While increasing the applied voltage during electrowetting experiments, a tip advances into the groove whose length continuously increases. The cross-section of such a tip decreases along the groove. This can be seen in Fig. 4(a) showing the close up of a liquid filament formed by electrowetting. From this, it is clear that the conductivity will be underestimated assuming a constant cross-section as done in our transmission line model.

Another consequence of this particular filament shape is that the liquid does not recede into the feeding drop when the applied voltage is ramped back to zero. Without any voltage applied, the liquid restores its material contact angle with the substrate, which is constant along the

Fig. 4. (a) Optical micrograph of a liquid filament in triangular grooves formed by electrowetting ($U_0 = 50\,\mathrm{V}$). (b) As the applied voltage is reduced to 0 V, filament breaks up into isolated droplets.

filament. The local Laplace pressure depends on the local filling height in the groove: at larger filling heights the Laplace pressure is smaller than at smaller filling heights. The filament is thus dynamically unstable and decays into isolated droplets, as shown in Fig. 4(b). This dynamic instability can be quantitatively understood by a linear stability analysis [15].

4 Conclusion

The appearance of static wetting morphologies in triangular grooves depend on wettability and groove geometry. By continuously varying the apparent contact angle, using the electrowetting effect, we can switch between different equilibrium morphologies. Thus liquid can be transported along prefabricated grooves from a reservoir at zero Laplace pressure. Due to the particular shape of the filament, the liquid cannot be drained from the grooves, but rather decays into isolated droplets.

This work was supported by the DFG priority program 1164 under grant number Se 1118/2. BL acknowledges support for this work through the U.S. National Science Foundation under grant number DMR-0603144.

References

1. C. Rascón, A.O. Parry, Nature **407**, 986 (2000)
2. M. Brinkmann, R. Blossey, Eur. Phys. J. E **14**, 79 (2004)
3. R. Seemann, M. Brinkmann, E.J. Kramer, F.F. Lange, R. Lipowsky, Proc. Nat. Acad. Sci. **102**, 1848 (2005)
4. K. Khare, S. Herminghaus, J.-C. Baret, B.M. Law, M. Brinkmann, R. Seemann, Langmuir **23**, 12997 (2007)
5. C. Quilliet, B. Berge, Europhys. Lett. **60**, 99 (2002)
6. T. Someya, A. Dodabalapur, A. Gelperin, H.E. Katz, Z. Bao, Langmuir **18**, 5299 (2002)
7. F. Mugele, J.-C. Baret, J. Phys.: Cond. Mat. **17**, R705 (2005)
8. G. Lippmann, Ann. Chimie Phys. **1875** 5^{e} séries, t. V
9. J. Sagiv, J. Am. Chem. Soc. **102**, 92 (1980)
10. J.-C. Baret, M. Decré, S. Herminghaus, R. Seemann, Langmuir **21**, 12218 (2005)
11. P. Concus, R. Finn, Proc. Nat. Acad. Sci. **63**, 292 (1969)
12. P. Concus, R. Finn, Acta. Math. **132**, 177 (1974)
13. J. Buehrle, S. Herminghaus, F. Mugele, Phys. Rev. Lett. **91**, 086101 (2003)
14. R. Shuttleworth, C.L.J. Bailey, Disc. Faraday Soc. **3**, 16 (1948)
15. K. Khare, M. Brinkmann, B.M. Law, E. Gurevich, S. Herminghaus, R. Seemann, Langmuir **23**, 12138 (2007)